Sensitivity Analysis for Prediction of Bead Geometry using Plasma Arc Welding in Bellows Segment

M. H. Park[1], I. S. Kim[2*], J. P. Lee[3], D. H. Kim[4], B. J. Jin[5], I. J. Kim[6], J. S. Kim[7]

[1,2,3,4,5]Department of Mechanical Engineering, Mokpo National University, 16, Dorim-ri, Chungkye-myun, Muan-gun, Jeonnam 534-729, South Korea

[6,7] Korea Institute of Industrial Technology, Cheomdan-venturero 108beon-gil, Buk-gu, Gwangju, 500-460 Republic of Korea

Abstract— *The automated welding systems, have received much attention in recent years, because they are highly suitable not only to increase the quality and productivity, but also to decrease manufacturing time and cost for a given product. To get the desired quality welds in automated welding system is challenging, an algorithm is needed that has complete control over the relevant process parameters in order to obtain the required bead geometry. However, there is still the lack of algorithms that can predict bead geometry over a wide range of welding conditions. Therefore, to solve this problem, this paper investigated the relationship between the process parameters and the bead geometry in Plasma arc welding (PAW). The quantitative effect of process parameters on bead geometry was calculated using sensitivity analysis. From the experimental results, the developed algorithm can predict the bead dimensions within 0–10% accuracy from analyzed parameters. It also showed that the change of process parameters affects the bead width relatively stronger than bead height.*

Keywords— Plasma Arc Welding, Bellows Segment, Sensitivity Analysis, Factorial Design, Optimization, Bead Geometry.

I. INTRODUCTION

Recently automated welding systems have received much attention because they are highly suitable not only to increase production rate and quality, but also to decrease cost and time to manufacture for a given product. To get the desired quality welds, it is essential to have complete control over the relevant process parameters in order to obtain the required bead geometry and which is also based on weldability. However, new algorithms need to be developed to make effective use of automated arc welding process.

Previous works on relationship between the process parameters and bead geometry in arc welding process can be grouped into two distinct areas: empirical methods based on studies of actual welding situations [1]-[2] and theoretical studies based on heat flow theory [3,4]. Despite the large number of attempts to analysis arc welding process, there is still the lack of algorithms that can predict bead geometry over a wide range of welding conditions. Sensitivity analysis, a method to identify critical parameters and rank them by their order of importance, is paramount in model validation where attempts are made to compare the calculated output to the measured data. This type of analysis can study which parameters must be most accurately measured, thus determining the input parameters exerting the most influence upon model outputs. It differs considerably from the usual approach of perturbing a process parameter of a known amount and evaluating the new results. Various statistical techniques such as regression analysis, Response Surface Methodology (RSM) and Taguchi method have been applied to modeling and optimization of bead geometry in Gas Metal Arc(GMA) welding[5]-[8]. Palani and Murugan[9] developed mathematical model for prediction of bead geometry in Flux Core Arc(FCA) welding using a RSM method. Taguchi method was also used to analyze the effect of each process parameter on the bead geometry [10]-[11]. Effect of pulse current on bead profiles of Gas Tungsten Arc(GTA) welded aluminum alloy joints has been studied [12]. Because the solution of a mathematical model to predict bead geometry is complex and the parameters involved are highly coupled, some researchers have resorted to Artificial Intelligence(AI) such as Artificial Neural Network(ANN) and Genetic Algorithm(GA) techniques based on large experimental databases [13]-[14]. Also, Son and Kwak [15] established a sensitivity formulation for eigen values, including repeated eigenvalues, with respect to the change of boundary conditions. The tangential design velocity component was employed to present the change of boundary conditions. The practical PAW process is widely appreciated in the aerospace, chemical, naval, nuclear industries, etc[16]. Prasada et al. investigated the weld quality characteristics of pulsed current micro-plasma arc welded austenitic stainless steels and considered weld pool geometry, microstructure, grain size, hardness and tensile properties as weld quality characteristics. It was established that SS 304L attained better weld quality characteristics at same welding conditions as compared to SS 316 L, SS 316Ti, SS 321[17].

Recently, Choi et al. [18] proposed sensitivity analysis for laser surface treatment by the differentiation of the analytic solution with respect to the laser beam radius and beam scanning velocity. It is evident that the qualitative and quantitative effectiveness of the process parameters can be determined using sensitivity analysis.

In this paper, investigation was carried out to study the relationship between the process parameters and the bead geometry in Plasma arc welding (PAW). The quantitative effect of process parameters on bead geometry was calculated using sensitivity analysis, and thus critical parameters can be identified and ranked by their order of importance.

II. PLASMA ARC WELDING PROCESS

Since PAW is an arc welding process similar to Gas Tungsten Arc (GTA) welding, the electric arc is formed between an electrode (which is usually but not always made of sintered tungsten) and the work piece. The key difference from GTA welding is that in PAW welding, by positioning the electrode within the body of the torch, the plasma arc can be separated from the shielding gas envelope. The plasma is then forced through a fine-bore copper nozzle which constricts the arc and the plasma exits the orifice at high velocities (approaching the speed of sound) and a temperature approaching 28,000 °C (50,000 °F) or higher. Experiments of bellows segment were conducted by plasma welder, in which there was an automatic welding system. Figure 1 shows the experimental setup of PAW process. The system mainly comprises the plasma welding power source, a shielding gas controller, a water-cooled controller and welding monitoring system. This experimental material was employed to deposit orbital welds on austenitic stainless steel 304 bellows segment with dimensions of an external diameter 64 mm, an inner diameter 39 mm and thickness 0.15 mm. The dimensions of bellows segment and the direction for plasma arc welding process on a test specimen are shown in Figure 2.

FIGURE 1 PLASMA ARC WELDING EXPERIMENTAL SETUP

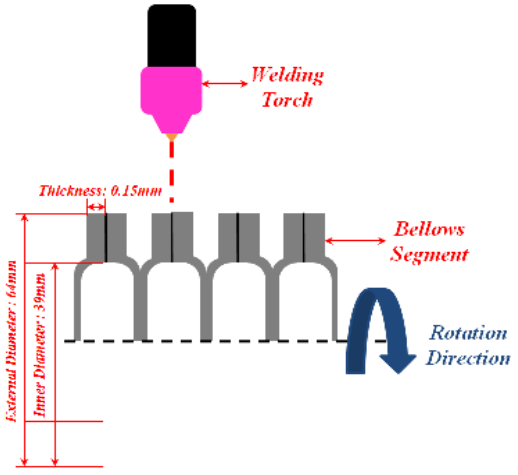

(A)A SCHEMATIC DIAGRAM FOR PAW PROCESS

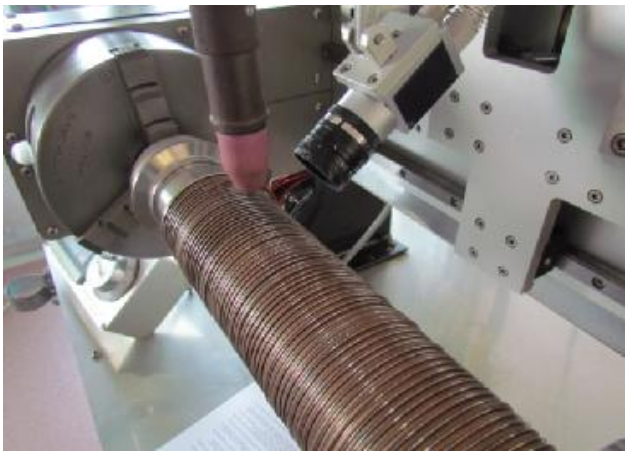

(B) EXPERIMENTAL OVERVIEW

FIGURE 2 OVERVIEW OF SPECIMEN WELDED USING PAW PROCESS

The chosen factors for this study were welding current, arc voltage and shielding gas ratio, and the responses were bead width and bead height as welding quality. The 2^3 factorial designs provided the main effect and interaction effects of three parameters at two levels. The process parameters and limits employed in this study are given in Table 1. All other parameters

except these parameters under consideration were fixed. Figure 3 illustrates a model of a process parameter with input and output parameters in PAW process. The factorial design required 8 weld runs for fitting each equation. This continued until the predetermined-factorial experimental runs were completed. To measure the bead geometry, transverse sections of each weld were cut using a power hacksaw from the mid-length position of the welds, and the end faces were machined. Specimen end faces were polished and etched using a 2.5%nital solution to display bead dimensions. The schematic diagram of bead geometry was employed as shown in Figure 4. The factorial matrix was assumed to link the mean values of the measured results with changes in the three process parameters for determining local features of the response surface. The experimental results were analyzed on the basis of relationships between process parameters and bead dimensions in the PAW process. The previous researches have studied the relationships between the underwater wet parameters and process stability [19]-[20]. In this study, the levels of the welding parameters are carefully set to make sure that the PAW processes are stable and can obtain good weld beads. The typical plasma arc welding bead appearances obtained in this study are shown in Table 2.

TABLE 1
PROCESS PARAMETERS AND LIMITS

Parameter	Symbol	Unit	Limits
Welding current	I	Amp	5, 6
Arc Voltage	V	Volt	12, 12.5
Shielding gas ratio	S	*l*/min	15, 18
Fixed parameters	Welding speed : 2CPM(Cm/min) CTWD : 2.5mm		

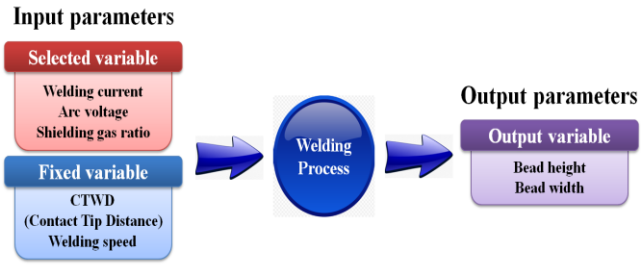

FIGURE 3 INPUT AND OUTPUT PARAMETERS OF THE PAW PROCESS

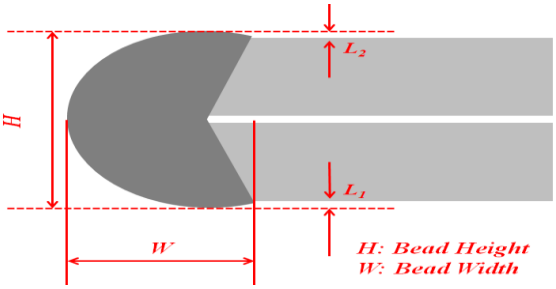

FIGURE 4 MEASUREMENT OF BEAD GEOMETRY

TABLE 2
BEAD GEOMETRY OF PAW PROCESS: CROSS SECTION

Test No.	Bead geometry	Test No.	Bead geometry
1	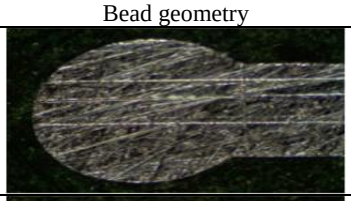	2	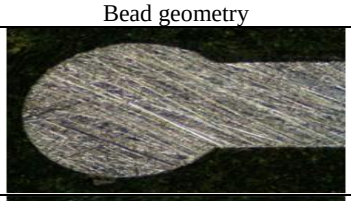
3		4	
5	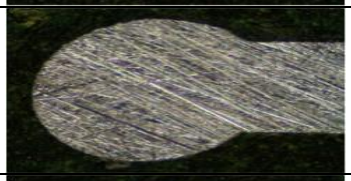	6	
7		8	

III. RESULTS AND DISCUSSION

Process parameters and the corresponding bead geometry of factorial matrix experiments for PAW process are presented in Table 3.

TABLE 3
EXPERIMENTAL LAYOUT USING 2^3 FACTORIAL MATRIX AND MEASURED BEAD GEOMETRY

Test No.	Process parameter			Bead geometry				
	I	V	S	W	H	L_1	L_2	L_1/L_2
1	5	12	15	3.306	3.270	0.537	0.595	1.114
2	5	12	18	3.620	3.075	0.364	0.705	1.937
3	5	12.5	15	3.620	3.273	0.719	0.731	1.017
4	5	12.5	18	3.623	3.306	0.348	0.817	2.348
5	6	12	15	3.608	3.174	0.558	0.731	1.310
6	6	12	18	3.757	2.963	0.545	0.595	1.092
7	6	12.5	15	3.757	2.690	0.347	0.769	2.216
8	6	12.5	18	4.174	2.901	0.331	0.796	2.405

3.1 Development of empirical models

Based on the results from the above factorial design, a curvilinear regression analysis was performed with the predictors that were found to be statistically significant against bead geometry. Suppose that the relationship between bead geometry as a dependent parameter and process parameters including welding current, arc voltage and the shielding gas ratio as independent parameters can be expressed by the following equation,

$$Y = b_1 (I)^{b2} (V)^{b3} (S)^{b4} \tag{1}$$

Where Y is the measured bead geometry in [mm], I is the welding current, V is the arc voltage, S is the shielding gas ratio. Also, b_1, b_2, b_3, and b_4 are curvilinear coefficients to be estimated for the model. This equation can be written as,

$$Y = b_1 + b_2 \ln I + b_3 \ln V + b_4 \ln S \tag{2}$$

Thus, the above equation can be expressed by the following linear mathematical form,

$$\eta = \beta_1 x_1 + \beta_2 x_2 + \beta_3 x_3 + \beta_4 x_4 \tag{3}$$

Where h is the logarithmic value of the experimentally measured response (bead geometry), β_1, β_2, β_3, β_4 are constants to be estimated, x_1, x_2, x_3, x_4 are logarithmic values of welding current, arc voltage and shielding gas ratio. The commercial statistical package SAS [19] was utilized for all the multiple regression analyses in this research. The procedure employed resulted in the following predictive equations;

Bead width:

$$W = \frac{V^{0.338}}{I^{0.247}\ S^{0.078}\ 10^{0.092}} \tag{4}$$

Bead height:

$$H = \frac{V^{0.587}}{I^{0.204}\ S^{0.064}\ 10^{0.872}} \tag{5}$$

The adequacy of the models and the significance of coefficients were tested by applying the analysis of variance technique and student's (T) test respectively. Table 4 shows the Standard Error of Estimates (SEE), coefficients of multiple correlations (R), and coefficients of determination (100R) for the above models respectively.

TABLE 4
ANALYSIS OF VARIANCE TESTS FOR MATHEMATICAL MODELS FOR BEAD GEOMETRY

Bead geometry	SE (Standard Error)	R^2(Coefficient of determination)	Adjusted R^2
Bead width	0.20470	89.8%	28.7%
Bead height	0.06859	98.6%	90.1%

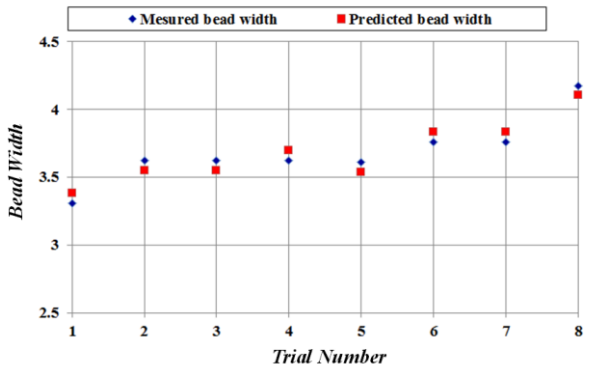

FIGURE 5 BEAD MODEL ANALYSIS GRAPH FOR BEAD WIDTH

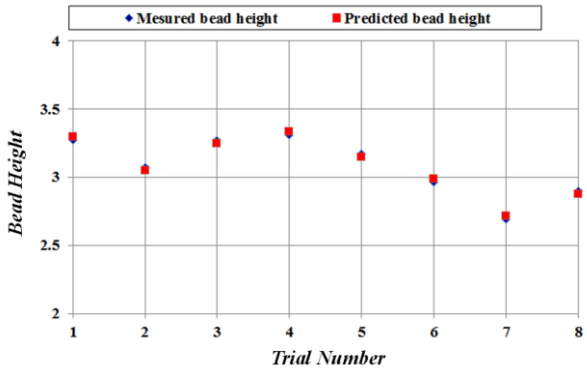

FIGURE 6 BEAD MODEL ANALYSIS GRAPH FOR BEAD HEIGHT

It is evident that all models were adequate. To ensure the accuracy of the developed equations and survey the spread of the values, results were again plotted using scatter graphs. These graphs of measured vs calculated values of bead dimensions are presented in Figures 5–6 for bead width and bead height respectively. The line of best fit for plotted points was also drawn using regression computation. Another criterion employed to judge the accuracy and efficiency of the developed models to predict bead geometry was the percentage deviation that is defined in Eq. (6). With this criterion, it would be much easier to see how the developed models fit and how close the predicted values are to the actual ones.

$$\lambda = \frac{R_A - R_E}{R_E} \times 100 \tag{6}$$

Where λ is percentage error, R_A is the calculated results and RE is the experimental results. It was decided to group these into six categories: 0–2%, 2–4%, 4–6%, 6–8%, 8–10% and over 10%. The results of this analysis for the bead geometry are presented in Figure 7. During analysis of the results, it was observed that the developed models for plasma arc welding yielded more accurate bead dimensions. The conclusion from the results of this analysis for the experimental runs is that the calculated results may predict the measured values with consistent accuracy.

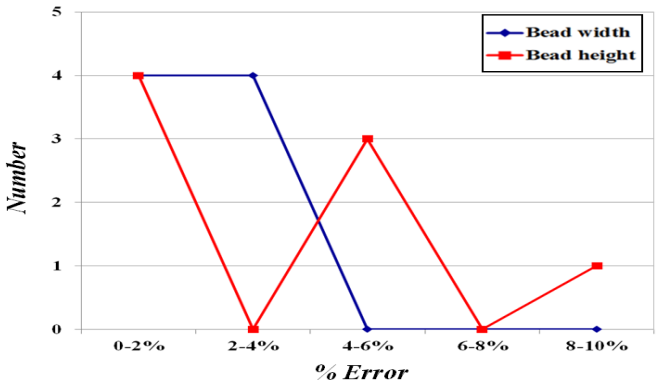

FIGURE 7 ACCURACY ANALYSES OF THE DEVELOPED EQUATIONS

3.2 Sensitivity analysis of empirical equation for bead geometry

From the above resultant equations for the estimation of bead geometry, the sensitivity equations are obtained by differentiation with respect to process parameters of interest such as welding current, arc voltage and shielding gas ratio that are explored here. To obtain the sensitivity equations for arc current, the Eqs. (4) and (5) were differentiated with respect to

welding current. The sensitivity equations are shown in Eqs. (7) and (8). They represent the sensitivity of bead width and height for welding current, respectively.

$$dW/dI = -0.247 I^{-1.247} V^{0.338} S^{-0.078} 10^{-0.092} \quad (7)$$

$$dH/dI = -0.204 I^{-1.204} V^{0.587} S^{-0.064} 10^{-0.872} \quad (8)$$

The sensitivity equations for arc voltage can be determined by differentiating Eqs. (4) and (5) with respect to arc voltage. They are shown in Eqs. (9) and (10).

$$dW/dV = 0.338 V^{-0.662} I^{-0.247} S^{-0.078} 10^{-0.092} \quad (9)$$

$$dH/dV = 0.587 V^{-0.413} I^{-0.204} S^{-0.064} 10^{-0.872} \quad (10)$$

And the sensitivity equations for shielding gas ratio are as follows;

$$dW/dS = -0.078 S^{-1.078} I^{-0.247} V^{0.338} 10^{-0.092} \quad (11)$$

$$dH/dS = -0.064 S^{-1.064} I^{-0.204} V^{0.587} 10^{-0.872} \quad (12)$$

The purpose of this investigation is to show the effectiveness of process parameters by using the direct sensitivity analysis technique on these empirical equations. Table 5 shows the applied welding parameters and the calculated results of sensitivity analysis such as welding current, arc voltage and shielding gas ratio. For these conditions, sensitivities of arc voltage on bead width are positive, and sensitivities of welding current and shielding gas ratio are negative. Also sensitivities of arc voltage on bead height are positive, and sensitivities of welding current and shielding gas ratio are negative. Depending on each of the calculated sensitivity results, an increasing and decreasing tendency was found for the bead height and width. In addition, it was found that as the welding current is reduced there is also reduction in the bead width and height; and it was also confirmed that if the arc voltage is increased the tendency of bead width and height also increases. Figure 8 shows the sensitivity of welding current on bead geometry (bead width and bead height) for various welding conditions. The bead width is more sensitive in the low welding current region but sensitivity of the bead height increases in the high arc voltage region. The sensitivities of arc voltage are represented in Figure 9. These results reveal that the bead width is more sensitive than bead height. It means that the variation of arc voltage causes small changes of bead height and large changes of bead width. Figure 10 shows the results of sensitivity analysis of shielding gas ratio. Generally, the sensitivity values of bead width are higher than bead height. This means that shielding gas ratio affects the bead width more strongly than bead height. The sensitivities of welding current and arc voltage on bead width are positive, but sensitivities of shielding gas ratio on bead geometry are negative. Since the sensitivity of welding current on bead width and bead height is much higher than that of shielding gas ratio, the change of welding current is more useful in control of bead width and bead height.

TABLE 5
BEAD GEOMETRY SENSITIVITIES OF PROCESS PARAMETERS

Welding parameters			Bead width sensitivities					
Welding current(A)	**Arc voltage(V)**	**Shielding gas ratio(*l*/min)**	***dW/dI***	***dW/dV***	***dW/dS***	***dH/dI***	***dH/dV***	***dH/dS***
5	12	15	-0.05036	0.02795	-0.00530	-0.01427	0.01682	-0.00149
5	12	18	-0.04965	0.02756	-0.00436	-0.01410	0.01662	-0.00123
5	12.5	15	-0.05106	0.02872	-0.00537	-0.01461	0.01710	-0.00153
5	12.5	18	-0.05034	0.02831	-0.00442	-0.01444	0.01691	-0.00126
6	12	15	-0.04012	0.02672	-0.00507	-0.01145	0.01620	-0.00144
6	12	18	-0.03955	0.02634	-0.00416	-0.01132	0.01602	-0.00118
6	12.5	15	-0.04068	0.02745	-0.00514	-0.01173	0.01648	-0.00147
6	12.5	18	-0.04010	0.02706	-0.00422	-0.01160	0.01629	-0.00121

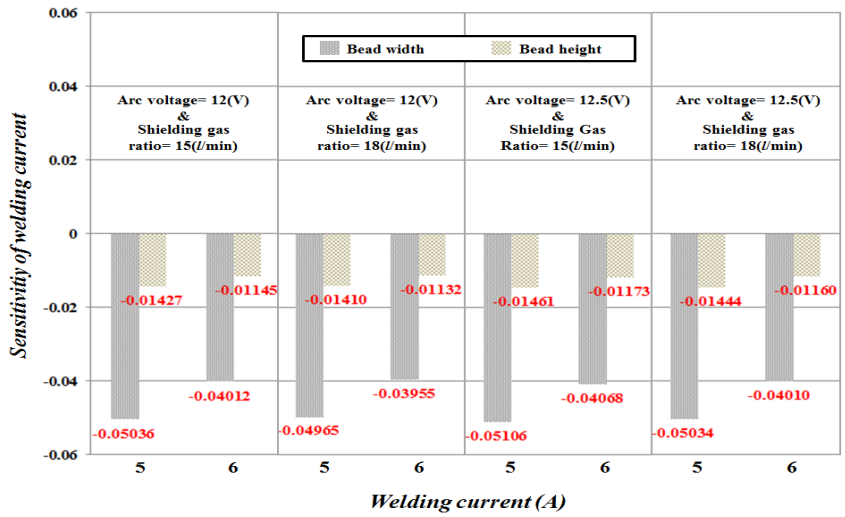

FIGURE 8 SENSITIVITY ANALYSIS RESULTS OF WELDING CURRENT

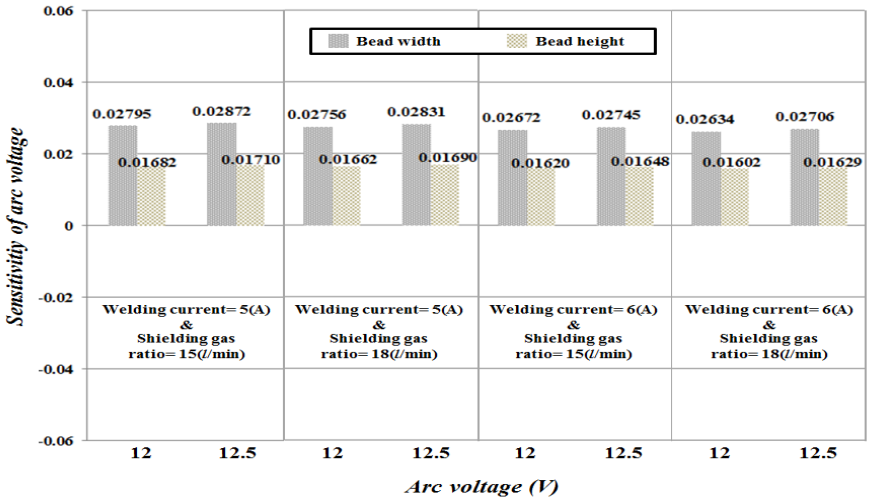

FIGURE 9 SENSITIVITY ANALYSIS RESULTS OF ARC VOLTAGE

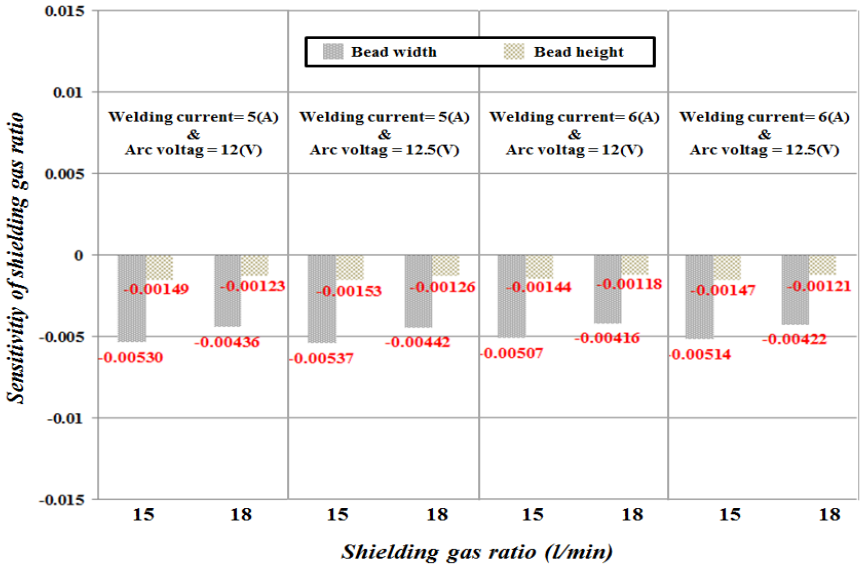

FIGURE 10 SENSITIVITY ANALYSIS RESULTS OF SHIELDING GAS RATIO

IV. CONCLUSION

In this paper, the selection of the process parameters for PAW process of austenitic stainless steel 304 bellows segment with bead geometry has been reported. The optimal bead geometry was chosen bead width and bead height. The factorial design has been adopted to solve the optimal bead geometry. Experimental results have shown that process parameters such as welding current, arc voltage and shielding gas ratio influence the bead width and bead height in PAW processes. Empirical models developed from the experimental data can be employed to study relationships between process parameters and bead geometry and to predict the bead dimensions within 0–10% accuracy. Sensitivity analysis has been investigated to represent the effectiveness of the processing parameters on these empirical equations and showed that the change of process parameters affects the bead width more strongly than bead height relatively. The developed models should be put into perspective with the standard plasma arc welding power source that was employed to conduct the experimental work. Factorial analysis has the potential for more stringent sensitivity analysis and may be used for optimal parameter estimation for other mathematical models.

ACKNOWLEDGEMENTS

This research was financially supported by the Ministry of Education (MOE) and National Research Foundation NRF) of Korea through the Human Resource Training Project for Regional Innovation. (No. 2013H1B8A2032082)

REFERENCES

[1] S. B. Jones, "Process tolerance in submerged arc welding," The Welding Institute Report, 1976, pp. 1–3.
[2] R. S. Chandel and S. R. Bala, "Effect of welding parameters and groove angle on the soundness of root beads deposited by the SAW process," Proceedings of the International Conference on Trends in Welding Research, 1986, pp. 379–385.
[3] T. Shinoda and J. Doherty, "The relationship between arc welding parameters and weld bead geometry," The Welding Institute Report, 1978, pp.74-76.
[4] D. K. Roberts and A. A. Wells, "Fusion welding of aluminium alloys," Br. Weld. J., vol. 1, 1954, pp. 553–559.
[5] K. Pal and S. K. Pal, "Soft computing methods used for the modelling and optimisation of gas metal arc welding," International Journal of Manufacturing Research, vol. 6(1), 2011, pp. 15−29.
[6] N. Murugan and R. S. Parmar, "Effects of MIG process parameters on the geometry of the bead in the automatic surfacing of stainless steel," Journal of Materials Processing, vol. 41(4), 1994, pp. 381–398.
[7] I. S. Kim, A. Basu and E. Siores, "Mathematical models for control of weld bead penetration in the GMAW process," International Journal of Advanced Manufacturing Technology, vol. 12(6), 1996, pp. 393–401.
[8] P. S. Rao, O. P. Gupta, S. N. Murty, and A. B. Rao, "Effect of process parameters and mathematical model for the prediction of bead geometry in pulsed GMA welding," International Journal of Advanced Manufacturing Technology, vol. 45(5), 2009, pp. 496–505.
[9] P. K. Palani and N. Murugan, "Development of mathematical models for prediction of weld bead geometry in cladding by flux cored arc welding," International Journal of Advanced Manufacturing Technology, vol. 30(7), 2006, pp. 669–676.
[10] S. Pal, S. K. Malviya, S. K. Pal and A. K. Samantaray, "Optimization of quality characteristics parameters in a pulsed metal inert gas welding process using grey-based Taguchi method," International Journal of Advanced Manufacturing Technology, vol. 44(11), 2009, pp. 1250−1260.
[11] Y. S. Tarng and W. H. Yang, "Optimization of the weld bead geometry in gas tungsten arc welding by the Taguchi method," International Journal of Advanced Manufacturing Technology, vol. 14(8), 1998, pp. 549–554.
[12] N. Karunakaran and V. Balasubramanian, "Effect of pulsed current on temperature distribution, weld bead profiles and characteristics of gas tungsten arc welded aluminum alloy joints," Transactions of Nonferrous Metals Society of China, vol. 21, 2011, pp. 278–286.
[13] I. S. Kim, J. S, Son, C. E. Park, I. J. Kim and H. H. Kim, "An investigation into an intelligent system for predicting bead geometry in GMA welding process," Journal of Materials Processing, vol. 159(1), 2005, pp. 113–118.
[14] L. Subashini and M. Vasudevan, "Adaptive neuro-fuzzy inference system (ANFIS)-based models for predicting the weld bead width and depth of penetration from the infrared thermal image of the weld pool," Metallurgical and Materials Transactions B, vol. 43(1), 2012, pp. 145–154.
[15] E. Friedman and S. S. Glickstein, "An investigation of the thermal response of stationary gas tungsten arc welds," Welding Journal, vol. 55(12), 1976, pp. 408–420.
[16] K. H. Tseng, S. T. Hsieh and C. C. Tseng, "Effect of process parameters of micro–plasma arc welding on morphology and quality in stainless steel edge joint welds," Sci Tech Weld Join, 2003, pp.423–430.
[17] K. S. Prasada, S. Rao and D. N. Rao, "An investigation on weld quality characteristics of pulsed current micro plasma arc welded austenitic stainless steels," Int J Eng Sci Tech, 2012, pp.159–168
[18] R. S. Chandel, "Mathematical modeling of gas metal arc weld features," Proceedings of the Fourth International Conference on Modeling of Casting and Welding Processes, April 1988, pp. 9–120.
[19] Y. F. Hsu and B. Rubinsky, "Two-dimensioanl heat transfer study on the keyhole plasma arc welding process," Int. J. Heat Mass Transfer, vol. 31, 1988, pp. 1409–1421.
[20] Y. D. Moon, I. K. Park, S. J. Hong and S. M. Cho, "The effect of clamping condition on melting efficiency in plasma arc welding of steel sheet," Proceedings of the 2007 Autumn Annual Meeting of Korean Welding Society, vol. 48, 2007, pp. 303–305.